Available online at www.sciencedirect.com
ScienceDirect
Journal of Solid State Chemistry 179 (2006) 3286–3294
JOURNAL OF SOLID STATE CHEMISTRY
www.elsevier.com/locate/jssc

Charge states of Ca atoms in β-dicalcium silicate

Kazuhiro Mori[a,*], Ryoji Kiyanagi[b], Masao Yonemura[c], Kenji Iwase[d,e], Takashi Sato[f], Keiji Itoh[a], Masaaki Sugiyama[a], Takashi Kamiyama[e], Toshiharu Fukunaga[a]

[a]*Research Reactor Institute, Kyoto University, Kumatori-cho, Sennan-gun, Osaka 590-0494, Japan*
[b]*Intense Pulsed Neutron Source Division, Argonne National Laboratory, Argonne, IL 60439, USA*
[c]*Institute of Applied Beam Science, Graduate School of Engineering and Science, Ibaraki University, 4-12-1 Nakanarusawa-cho, Hitach, Ibaraki 316-8511, Japan*
[d]*Department of Materials Structure Science, Graduate University for Advanced Studies, Tsukuba, Ibaraki 305-0801, Japan*
[e]*Institute of Materials Structure Science, High Energy Accelerator Research Organization, Tsukuba, Ibaraki 305-0801, Japan*
[f]*Department of Engineering Physics and Mechanics, Kyoto University, Kyoto 606-8501, Japan*

Received 18 May 2006; received in revised form 7 June 2006; accepted 10 June 2006
Available online 23 June 2006

Abstract

In order to study the crystal structure of β-Ca_2SiO_4, time-of-flight neutron powder diffraction experiments were carried out at temperatures between room temperature (RT) and 600 °C. Rietveld refinement at RT has shown that β-Ca_2SiO_4 is monoclinic based on $P2_1/n$ symmetry and two different types of Ca sites, Ca(1) and Ca(2). All interatomic distances within 3 Å were calculated, with the valences of Ca(1) with seven Ca–O bonds and Ca(2) with eight were estimated to be 1.87+ and 2+ by the Zachariasen–Brown–Altermatt formula (bond valence sum). Applying charge neutrality the two charge states of Ca in β-Ca_2SiO_4 are $[Ca(1)SiO_4]^{2-}$ and $Ca(2)^{2+}$, respectively. Furthermore, the $[Ca(1)SiO_4]^{2-}$ unit has the shortest Ca–O distance, and its length kept constant at 2.23 Å at all temperatures. In the short-range structure analysis at RT, the shortest Ca–O bond was also observed in a radial distribution function. These results imply that the $[Ca(1)SiO_4]^{2-}$ unit has covalency on the shortest Ca–O in addition to Si–O.

Keywords: β-Ca_2SiO_4; Crystal structure; Short-range structure; Neutron powder diffraction; Radial distribution function; Rietveld analysis; Bond valence sum

1. Introduction

Dicalcium silicate (Ca_2SiO_4) is a principal component in low heat portland cement (LHPC) and ordinarily portland cement that are frequently utilized for constructing huge concrete buildings. It is well known that the Ca_2SiO_4 adopts five forms depending on temperature, T: γ-phase ($T<500$ °C), β-phase (630 °C $<T<$ 680 °C), α'_L-phase ($T\sim$870 °C), α'_H-phase ($T\sim$1160 °C) and α-phase ($T\sim$1450 °C) [1–3]. Among these phases, the β-Ca_2SiO_4 has attracted much attention because this phase stably exists in cement clinkers even at room temperature (RT) [4]. The advanced structural investigations of β-Ca_2SiO_4 have been performed using X-ray and neutron powder diffractions [2–5]. In crystal structure refinements, it has been revealed that β-Ca_2SiO_4 has monotonic on the basis of $P2_1/n$ symmetry.

It is easily expected that advantages of concrete such as compressive strength and durability are strongly associated with cement hydration properties, which should be mostly characterized by the hydration properties of calcium silicate in cement clinkers. For example, the hydration properties of β-Ca_2SiO_4 affect the low heat of hydration in LHPC and the suppression of the self-contraction in concrete. The overall chemical reaction of β-Ca_2SiO_4 would be represented as follows:

$$\beta\text{-}Ca_2SiO_4 + (2+y-x)H_2O \rightarrow (CaO)_x(SiO_2)(H_2O)_y + (2-x)Ca(OH)_2, \quad (1)$$

where x and y are the Ca to Si ratios and the bound water contents in calcium silicate hydrate gel (C–S–H gel),

*Corresponding author. Fax: +81 724 51 2635.
E-mail address: kmori@rri.kyoto-u.ac.jp (K. Mori).

0022-4596/$ - see front matter © 2006 Elsevier Inc. All rights reserved.
doi:10.1016/j.jssc.2006.06.018

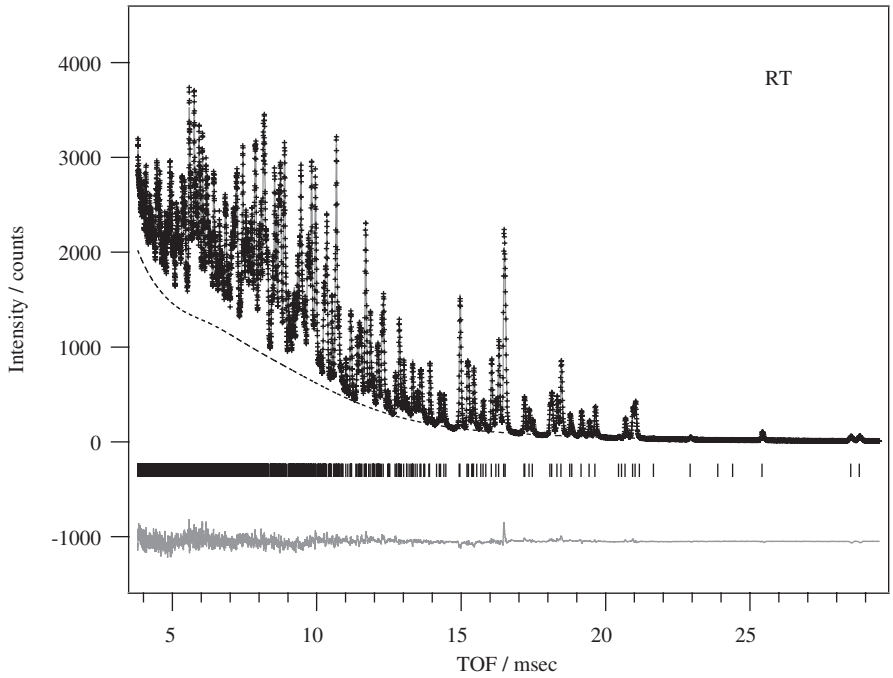

Fig. 1. Full pattern of Rietveld analysis result for β-Ca_2SiO_4 at RT. The plus marks are the observed neutron diffraction intensities, and the solid gray line is the calculated one. The vertical marks below the profile indicate the positions of the Bragg reflections. The curve at the bottom is the difference between the observed and calculated intensities.

respectively. The second term on the right-hand side of Eq. (1) is a calcium hydroxide ($Ca(OH)_2$). It has been believed that the hydration of calcium silicate proceeds in three steps [6–8]. In the first step, the calcium silicate and water dissolve into some kinds of ions; Ca^{2+}, OH^- and $H_2SiO_4^{2-}$. When ion concentrations are sufficient in water, the creation of C–S–H gel occurs. Furthermore, the exceeding Ca^{2+} ions are utilized to precipitate $Ca(OH)_2$. In such a hydration process, it is extremely important how Ca atoms in β-Ca_2SiO_4 dissolve in water. However, it seems that the mechanism of the solubility of Ca is not sufficiently discussed from a structural point of view; for instance, several different types of Ca sites in the crystal structure of β-Ca_2SiO_4 will be strongly concerned with the solubility of Ca.

In the present paper, we focus on the RT crystal structure of β-Ca_2SiO_4 studied using time-of-flight neutron powder diffraction (TOF-NPD) with Rietveld analysis coupled with radial distribution analysis. High-temperature NPD was utilized to examine the hydration process of β-Ca_2SiO_4.

2. Experimental

Although the elemental substitution is usually performed to stabilize β-Ca_2SiO_4 at RT, we applied the following sample preparation process to avoid the $\beta \rightarrow \gamma$ transformation in place of the elemental substitution [9]. The polycrystalline β-Ca_2SiO_4 was synthesized by conventional ceramic processing from $CaCO_3$ (99.99%) and SiO_2

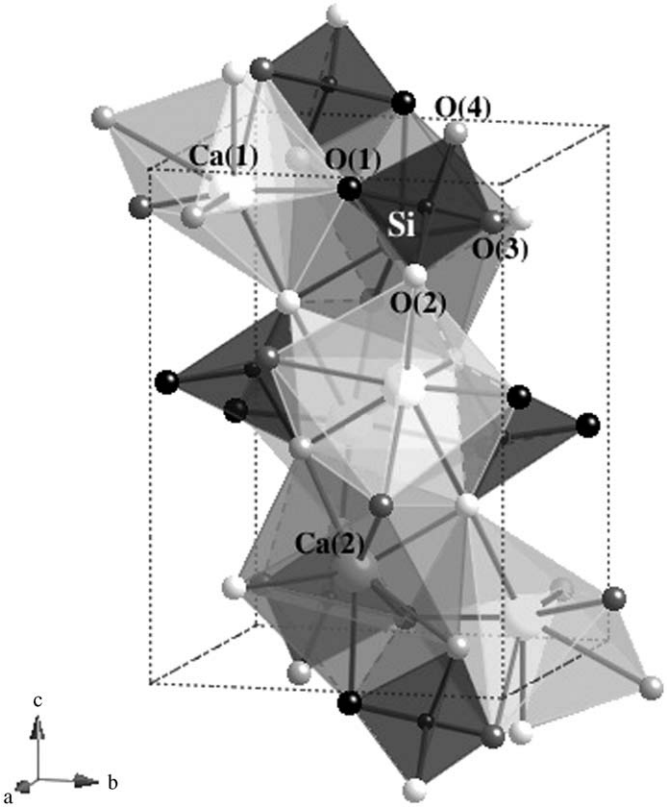

Fig. 2. Schematic illustration of β-Ca_2SiO_4 obtained from the result of Rietveld analysis at RT. The [SiO_4] tetrahedra are indicated in dark gray. Two gray polyhedra show [$Ca(1)O_7$] and [$Ca(2)O_8$], respectively.

(99.9%) powders which were well mixed in the molar proportion. The mixture was heated at 900 °C for 12 h in air. After grinding, the sample was pressed into disks (10 mm in diameter and about 1 mm in thickness) and heated at 1200 °C for 20 h in air to make it more uniform. The products were ground and reacted at 1200 °C for 6 h in air, followed by gradual cooling to 680 °C before quenching in air. The obtained Ca_2SiO_4 sample was checked by the X-ray powder diffractometer with Cu source (Rigaku Corporation, RAD-C). Eventually, we could confirm that no γ-Ca_2SiO_4 exists in this sample.

TOF measurements of β-Ca_2SiO_4 were carried out using the special environment powder diffractometer (SEPD), installed at the intense pulsed neutron source (IPNS) at the Argonne National Laboratory (ANL) [10]. Diffracted neutrons are detected by ^{3}He proportional counters installed in a back-scattering detector bank with 2θ-range of $\pm 145^\circ$. The resolution of the SEPD, $\Delta d/d$, is $\sim$0.34%, where d is the d-spacing. The powder sample was put into a cylindrical vanadium cell that has a diameter of 11.1 mm and a height of 70 mm. The TOF-NPD data were collected at RT (26 °C), 100, 200, 300, 400, 500 and 600 °C using the

Table 1
Refined structure parameters of β-Ca_2SiO_4

Atom	g	x	y	z	$U_{iso}/\times 10^2$ Å^2
(a) *At RT*					
Ca(1)	1	0.22713(21)	0.34205(20)	0.43014(15)	0.773(30)
Ca(2)	1	0.22040(25)	0.99706(23)	0.70239(14)	0.795(32)
Si	1	0.26655(27)	0.78183(17)	0.41734(15)	0.384(32)
O(1)	1	0.21702(19)	0.01223(16)	0.44055(12)	1.033(33)
O(2)	1	0.47902(20)	0.74878(17)	0.30783(11)	0.828(27)
O(3)	1	0.01437(19)	0.66726(18)	0.36274(12)	0.894(29)
O(4)	1	0.34546(19)	0.67176(20)	0.57325(11)	0.890(26)
$a = 5.50684(10)$ Å, $b = 6.74839(13)$ Å, $c = 9.30320(18)$ Å, $\beta = 94.590(1)^\circ$, $\chi^2 = 3.592$, $R_{wp} = 3.31\%$					
(b) *At 100 °C*					
Ca(1)	1	0.22758(26)	0.34135(23)	0.43000(18)	0.938(35)
Ca(2)	1	0.22175(30)	0.99676(27)	0.70249(17)	0.974(39)
Si	1	0.26642(31)	0.78222(20)	0.41725(17)	0.357(37)
O(1)	1	0.21738(23)	0.01188(19)	0.44026(15)	1.190(38)
O(2)	1	0.47955(24)	0.74831(21)	0.30788(14)	1.002(31)
O(3)	1	0.01452(23)	0.66792(21)	0.36280(15)	1.055(34)
O(4)	1	0.34420(22)	0.67173(23)	0.57329(13)	1.062(32)
$a = 5.51072(5)$ Å, $b = 6.75416(6)$ Å, $c = 9.31416(9)$ Å, $\beta = 94.474(1)^\circ$, $\chi^2 = 2.195$, $R_{wp} = 3.77\%$					
(c) *At 200 °C*					
Ca(1)	1	0.22771(28)	0.34057(25)	0.43005(19)	1.233(40)
Ca(2)	1	0.22183(32)	0.99671(29)	0.70254(18)	1.168(44)
Si	1	0.26571(33)	0.78225(21)	0.41712(19)	0.466(41)
O(1)	1	0.21796(25)	0.01171(20)	0.44008(16)	1.511(44)
O(2)	1	0.47933(26)	0.74769(23)	0.30802(15)	1.325(36)
O(3)	1	0.01483(25)	0.66838(23)	0.36257(16)	1.378(39)
O(4)	1	0.34279(24)	0.67164(25)	0.57327(14)	1.396(38)
$a = 5.51604(5)$ Å, $b = 6.76202(6)$ Å, $c = 9.32923(10)$ Å, $\beta = 94.313(1)$ o, $\chi^2 = 2.191$, $R_{wp} = 3.78\%$					
(d) *At 300 °C*					
Ca(1)	1	0.22895(28)	0.33965(25)	0.42985(20)	1.488(42)
Ca(2)	1	0.22272(31)	0.99630(29)	0.70267(18)	1.471(46)
Si	1	0.26542(32)	0.78254(21)	0.41710(19)	0.674(43)
O(1)	1	0.21858(24)	0.01128(19)	0.43970(16)	1.760(45)
O(2)	1	0.47955(26)	0.74709(22)	0.30875(16)	1.611(38)
O(3)	1	0.01568(24)	0.66921(23)	0.36232(16)	1.744(41)
O(4)	1	0.34115(24)	0.67220(24)	0.57290(13)	1.687(41)
$a = 5.52186(5)$ Å, $b = 6.77033(6)$ Å, $c = 9.34577(9)$ Å, $\beta = 94.139(1)^\circ$, $\chi^2 = 3.575$, $R_{wp} = 3.47\%$					
(e) *At 400 °C*					
Ca(1)	1	0.22922(34)	0.33906(30)	0.42927(24)	1.756(55)
Ca(2)	1	0.22423(38)	0.99628(35)	0.70234(23)	1.849(60)
Si	1	0.26421(39)	0.78248(25)	0.41757(23)	0.910(55)
O(1)	1	0.21908(30)	0.01131(24)	0.43968(19)	2.113(59)
O(2)	1	0.48050(33)	0.74660(27)	0.30938(20)	2.047(51)
O(3)	1	0.01564(29)	0.66999(29)	0.36124(20)	2.159(54)
O(4)	1	0.33960(29)	0.67286(30)	0.57230(16)	2.102(56)
$a = 5.52794(6)$ Å, $b = 6.77878(7)$ Å, $c = 9.36312(11)$ Å, $\beta = 93.952(1)^\circ$, $\chi^2 = 2.383$, $R_{wp} = 3.94\%$					

Table 1 (*continued*)

Atom	*g*	*x*	*y*	*z*	$U_{iso}/\times 10^2$ Å^2
(f) *At 500 °C*					
Ca(1)	1	0.23103(38)	0.33828(32)	0.42874(26)	2.025(63)
Ca(2)	1	0.22596(43)	0.99582(38)	0.70284(24)	2.214(69)
Si	1	0.26364(41)	0.78308(27)	0.41755(24)	1.183(63)
O(1)	1	0.21901(33)	0.01077(25)	0.43929(21)	2.405(66)
O(2)	1	0.48061(35)	0.74620(29)	0.31044(21)	2.267(56)
O(3)	1	0.01637(31)	0.67101(32)	0.36059(20)	2.579(62)
O(4)	1	0.33793(31)	0.67330(32)	0.57215(18)	2.347(63)
$A = 5.53414(6)$ Å, $b = 6.78699(8)$ Å, $c = 9.38074(11)$ Å, $\beta = 93.755(1)^\circ$, $\chi^2 = 2.357$, $R_{wp} = 3.94\%$					
(g) *At 600 °C*					
Ca(1)	1	0.23270(38)	0.33767(31)	0.42840(26)	2.469(66)
Ca(2)	1	0.22769(43)	0.99465(38)	0.70230(24)	2.704(72)
Si	1	0.26343(41)	0.78330(28)	0.41774(24)	1.571(65)
O(1)	1	0.22022(34)	0.01001(26)	0.43828(21)	3.015(69)
O(2)	1	0.48092(34)	0.74595(28)	0.31106(20)	2.549(57)
O(3)	1	0.01629(30)	0.67223(32)	0.35980(19)	3.065(66)
O(4)	1	0.33537(30)	0.67431(31)	0.57125(17)	2.765(64)
$A = 5.54076(6)$ Å, $b = 6.79576(8)$ Å, $c = 9.40045(10)$ Å, $\beta = 93.524(1)^\circ$, $\chi^2 = 3.560$, $R_{wp} = 3.52\%$					

Table 2
Important bond lengths between Ca and O at RT

Ca(1)–O		Ca(2)–O	
Ca(1)–O(1)	2.2287(15) Å	Ca(2)–O(1)	2.4367(18) Å
Ca(1)–O(1)	—	Ca(2)–O(1)	2.6575(18) Å
Ca(1)–O(2)	2.4869(18) Å	Ca(2)–O(2)	2.3907(20) Å
Ca(1)–O(2)	2.8818(18) Å	Ca(2)–O(2)	2.3855(19) Å
Ca(1)–O(3)	2.5426(18) Å	Ca(2)–O(3)	2.6542(21) Å
Ca(1)–O(3)	2.4281(18) Å	Ca(2)–O(3)	2.3852(17) Å
Ca(1)–O(4)	2.6475(18) Å	Ca(2)–O(4)	2.6209(20) Å
Ca(1)–O(4)	2.3582(16) Å	Ca(2)–O(4)	2.4493(18) Å

Howe Furnace. The crystal structure of β-Ca_2SiO_4 was determined by the Rietveld analysis program, GSAS, with the EXPGUI interface [11–13].

The local structure of β-Ca_2SiO_4 was investigated with the high-intensity total scattering spectrometer (HIT-II) at the pulsed neutron source of Neutron Science Laboratory (KENS) at the High Energy Accelerator Research Organization (KEK) [14–16]. The sample was loaded into a cylindrical Ti–Zr null-alloy cell that is 8.0 mm in inner diameter, 80 mm in height and 0.3 mm in thickness. The TOF-NPD pattern was measured at RT, and then the intensity data were corrected for background, absorption, multiple and incoherent scatterings to obtain the structure factor, $S(Q)$, where Q is the momentum transfer ($= 4\pi \sin\theta/\lambda$) [17,18]. The radial distribution function, RDF(r), was derived from the Fourier transformation of the $S(Q)$ measured up to $Q = 45$ Å^{-1}.

3. Results and discussion

Fig. 1 shows the TOF-NPD pattern of β-Ca_2SiO_4 at RT. The structure parameters were refined on the basis of $P2_1/n$

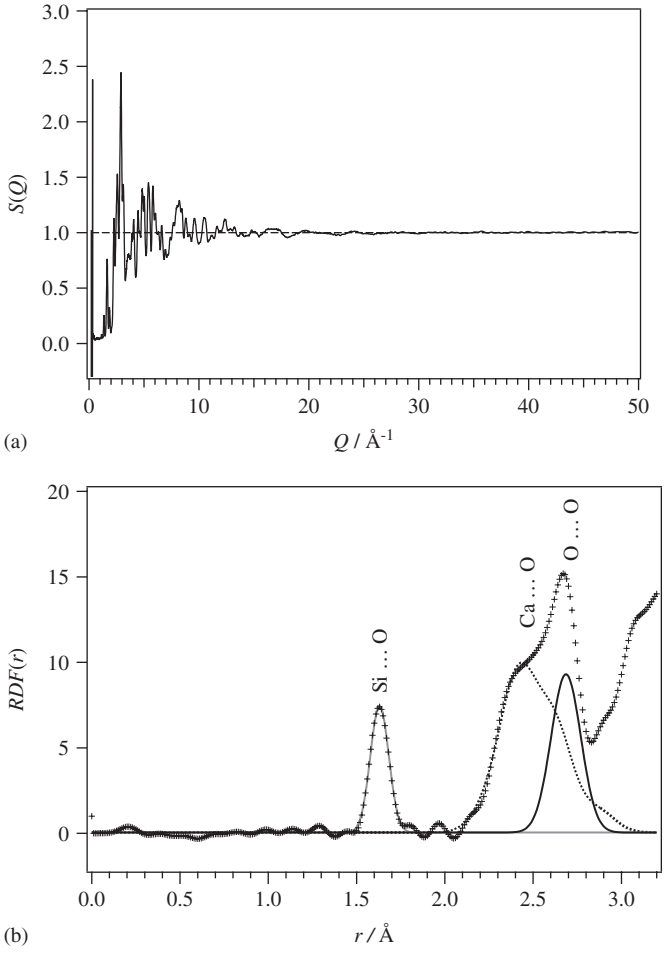

Fig. 3. Structure factor, $S(Q)$, (a) and radial distribution function, RDF(r), (b) of β-Ca_2SiO_4, respectively. In frame (b) the plus marks show the RDF(r). The gray solid line at around 1.6 Å, the gray broken one at around 2.4 Å and the black solid line at around 2.7 Å correspond to Si–O, Ca–O and O–O bonds.

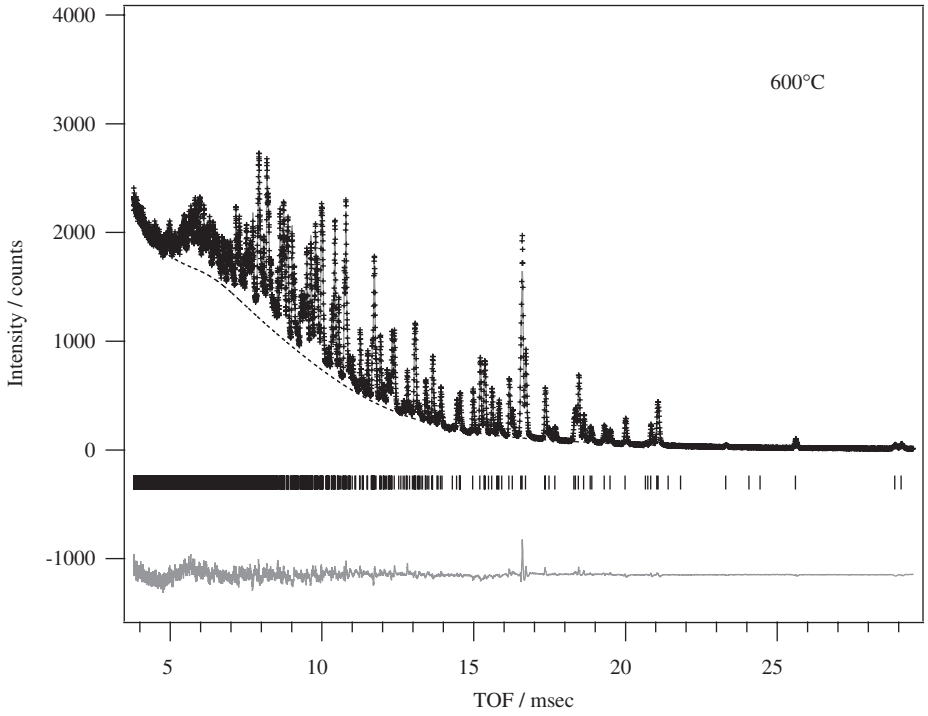

Fig. 4. Rietveld refinement pattern of β-Ca_2SiO_4 at 600 °C.

symmetry (monoclinic). In the Rietveld analysis occupancies at all atomic sites were fixed at unity. The intensity of background is fairly high, caused by incoherent scattering of vanadium due to a vanadium heater in the Howe Furnace. Nevertheless, an excellent fit between the observed and calculated patterns was obtained; $\chi^2 = 3.59$ and $R_{wp} = 3.31\%$, respectively. The crystal structure of β-Ca_2SiO_4 is illustrated in Fig. 2. The lattice parameters of β-Ca_2SiO_4 were estimated as follows: $a = 5.50684(10)$ Å, $b = 6.74839(13)$ Å, $c = 9.30320(18)$ Å and $\beta = 94.590(1)^\circ$. The refined structure parameters at RT are summarized in Table 1(a). Furthermore, the bond lengths between Ca and O are listed in Table 2. It is noteworthy that β-Ca_2SiO_4 has two different types of Ca sites; Ca(1) and Ca(2). The arrangements of oxygen atoms around Ca(1) and Ca(2) are markedly different, as can be seen in Fig. 2. The coordination numbers around Ca(1) and Ca(2) were calculated to be 7 and 8 within 3 Å of bond length, respectively. In addition, the Ca(1)–O bonds are widely distributed between 2.23 and 2.88 Å, while those of Ca(2)–O are converged between 2.39 and 2.66 Å. Especially, the Ca(1)–O(1), of which distance is 2.2287(15) Å, is the shortest bond in all Ca–O.

The RDF method gives the atomic arrangement in real space by just a Fourier transformation of the diffraction data. Fig. 3(a) shows the $S(Q)$ of β-Ca_2SiO_4 measured by the HIT-II. Also, the $RDF(r)$ of β-Ca_2SiO_4 derived from the Fourier transformation of the $S(Q)$ is shown in Fig. 3(b). In the RDF(r) the first peak at around 1.6 Å indicates Si–O bonds in a [SiO_4] tetrahedron. The coordination number calculated from the area of the first peak informs us that 4 oxygen atoms exist around Si. The second (r~2.4 Å) and third (r~2.7 Å) peaks correspond to Ca–O and O–O bonds, respectively. These peaks are assigned to the specific bonds using data provided by the Rietveld analysis, and not through using the RDF alone. As shown in Fig. 3(b), the peak of O–O could be described by a Gaussian function since the coordination number of O–O is 3 in the [SiO_4] tetrahedron. Consequently, the asymmetric and broad distribution in Ca–O bonds was recognized the result, and we could validate that the shortest Ca–O bond, Ca(1)–O(1), appreciably exists at around 2.23 Å in the $RDF(r)$.

Fig. 4 shows the TOF-NPD pattern of β-Ca_2SiO_4 at 600 °C. In the structure analysis, we also applied $P2_1/n$ symmetry to all TOF-NPD data above RT, where the profile parameters were fixed at the same values obtained from the Rietveld refinement at RT. As can be seen in Fig. 4, the good fit was obtained between the observed and calculated patterns; $\chi^2 = 3.56$, $R_{wp} = 3.52\%$. The structure parameters for each temperature are listed in Table 1. The temperature dependences of lattice parameters, a, b, c and β, are shown in Fig. 5. It was found that a, b and c linearly increase with decreasing β due to the thermal expansion. Fig. 6 summarizes the bond length for each bond and the bond angle of Ca(1)–O(1)–Si as a function of T. In frame (c) the [SiO_4] tetrahedron, which consists of four Si–O bonds, is hardly distorted at all temperatures. In contrast, the Ca(2)–O bond lengths except Ca(2)–O(4) at around 2.6 Å monotonically increase with raising T. Even though almost all of the Ca(1)–O bonds show the tendency to expand with increasing T, the bond length of Ca(1)–O(1) is

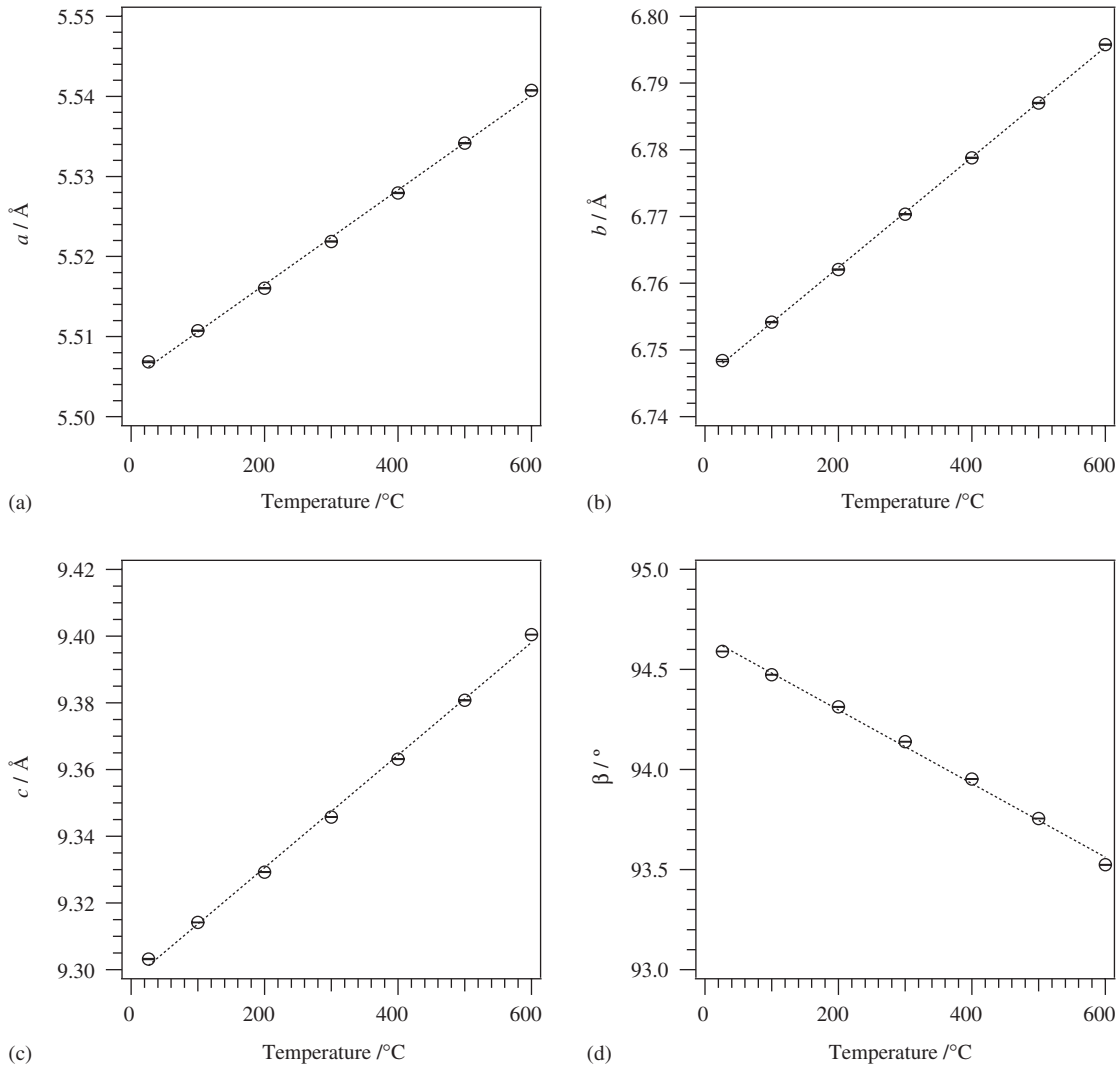

Fig. 5. Variation of lattice parameters as a function of T: (a) a, (b) b, (c) c and (d) β. The broken straight lines are guides to the eyes.

kept constant at 2.23 Å. On the other hand, the bond angle of Ca(1)–O(1)–Si increases with raising T, as shown in Fig. 6(d).

The Zachariasen–Brown–Altermatt formula (bond valence sum), that relates a bond length and a bond valence, is significantly beneficial to evaluate the valence for each Ca site [19–21]. The valence of Ca, V_{Ca}, is defined by the following equation:

$$V_{Ca} = \sum_i \exp\{(l_{Ca\text{-}O} - l_i)/B\}, \quad (2)$$

where i corresponds to the coordination number for each Ca site, $l_{Ca–O}$ is the bond valence parameter (= 1.967 Å) and $B = 0.37$ Å. Inserting the obtained Ca–O correlation lengths, l_i, in Eq. (2), $V_{Ca(1)}$ and $V_{Ca(2)}$ were estimated to be 1.868 and 1.997, respectively. From this result, Ca(2) could be safely regarded as Ca^{2+}, whereas the valence of Ca(1) is obviously less than 2+. As considering charge neutrality, it is most likely that the [SiO_4] tetrahedron provides the exceeding charge to Ca(1), that is, $Ca(1)^{1.87+}$–$[SiO_4]^{3.87-}$. This means that covalency exists in the Ca(1)–[SiO_4] unit, as shown in Fig. 7. In particular, we point out that there is a pathway providing the exceeding charge on the Ca(1)–O(1), because the bond length of Ca(1)–O(1) is considerably shorter than that of other Ca–O as demonstrated in the Rietveld and RDF analyses. Such a charge state of Ca(1) may cause the appearance of the shortest O–Si bond, O(1)–Si, in the [SiO_4] tetrahedron, as shown in Fig. 6(c). Moreover, the results obtained from the TOF-NPD experiments at high temperature would support that the Ca(1)–O(1) has covalency; the bond length of Ca(1)–O(1) did not change at all temperatures as well as Si–O bonds with strong covalency.

In recent investigations of C–S–H gels, the detailed crystal structures of Al-substituted 11 Å-tobermorite ($Ca_{4.9}Si_{5.5}Al_{0.5}O_{16.3}(OH)_{0.7}\cdot 5H_2O$), 14 Å-tobermorite ($Ca_4H_4Si_6O_{18}\cdot 8H_2O$) and jennite ($Ca_8H_4Si_6O_{18}(OH)_8\cdot 6H_2O$) have been reported by various authors [22–25]. As a structure common to all, they have a layered structure based on a Ca–O polyhedral sheet flanked on each side by liner silicate chains. However, as can be seen in Fig. 2, it seems that the [SiO_4] tetrahedra are isolated with Ca atoms in β-Ca_2SiO_4,

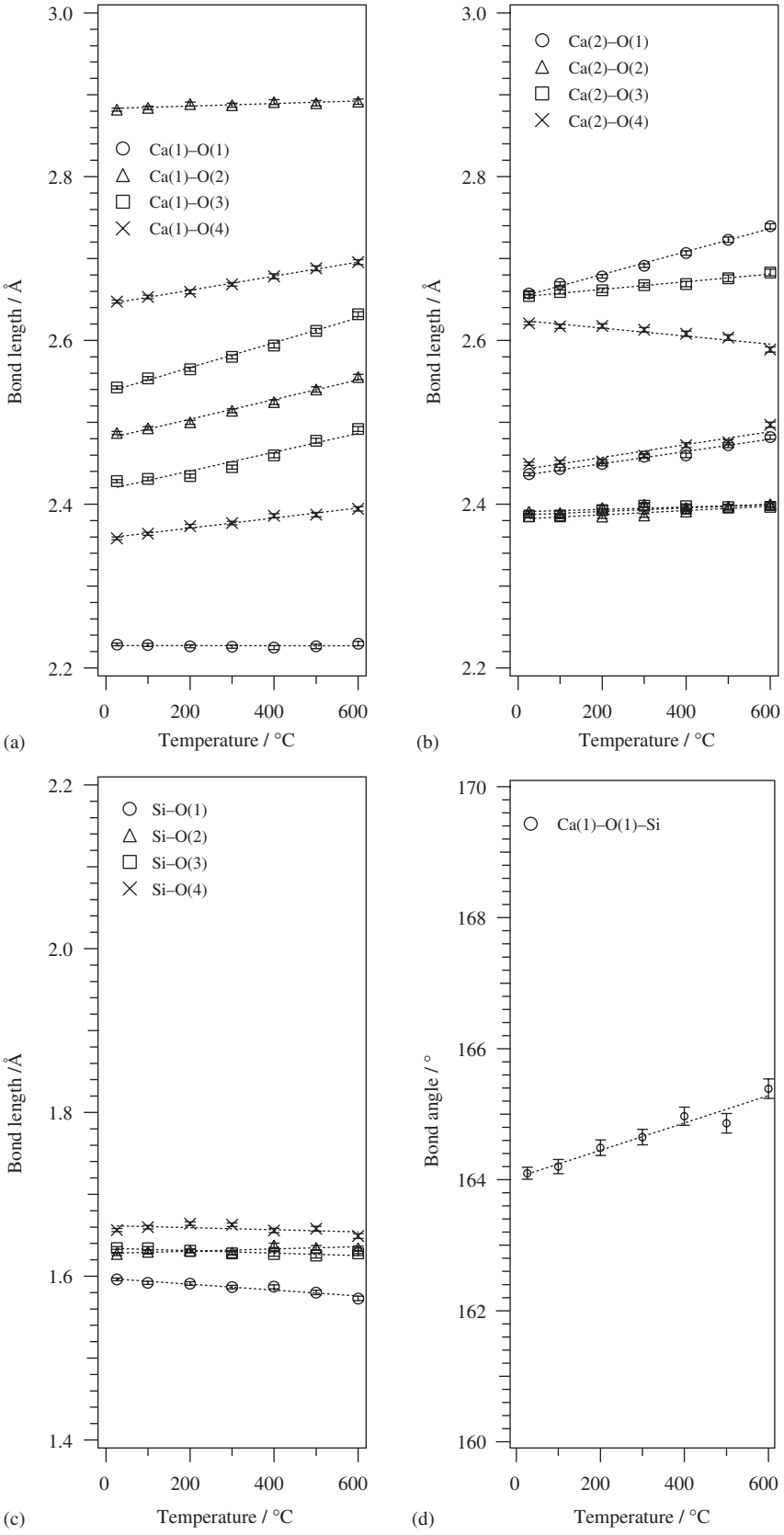

Fig. 6. Temperature dependences of: (a) Ca(1)–O bond lengths, (b) Ca(2)–O, (c) Si–O and (d) Ca(1)–O(1)–Si bond angle. The broken straight lines are guides to the eyes.

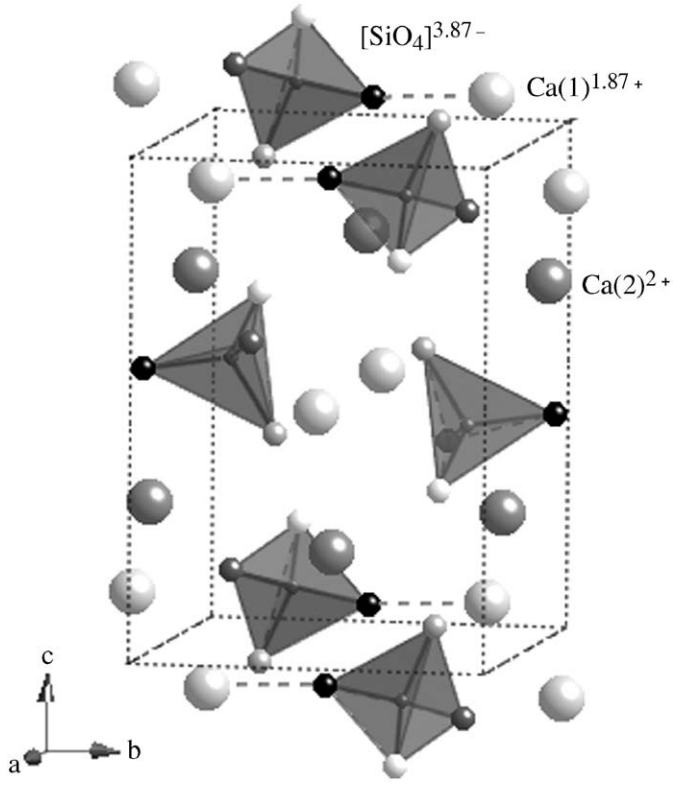

Fig. 7. Charge state model in β-Ca_2SiO_4. Two types of charge states are demonstrated; $Ca(1)^{1.87+}$–$[SiO_4]^{3.87-}$ unit and $Ca(2)^{2+}$.

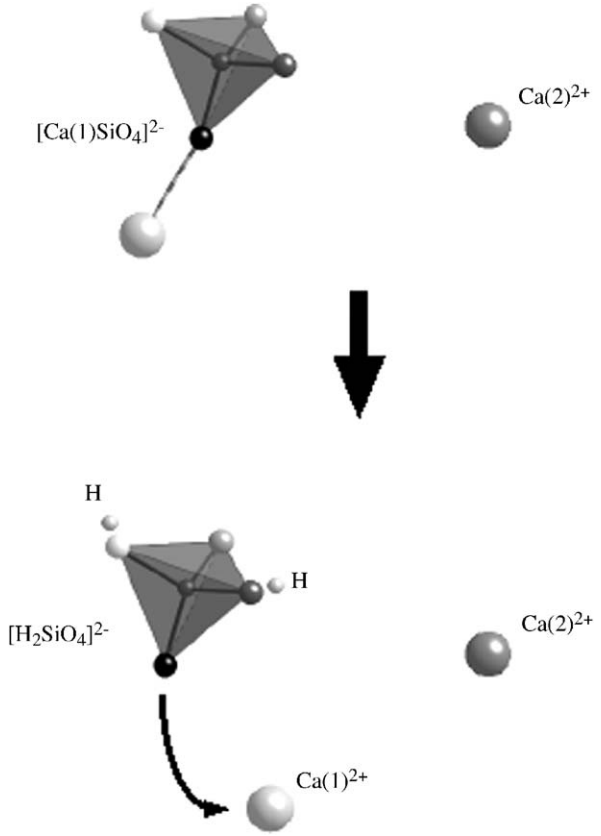

Fig. 8. Image of intermediate state during the hydration process of β-Ca_2SiO_4. The $[Ca(1)SiO_4]^{2-}$ unit is transformed to $[H_2SiO_4]^{2-}$ by the substitution of Ca(1) with two protons. In contrast, Ca(2) maintains condition of Ca^{2+} in water.

namely no silicate chains exist. Similarly, the isolated $[SiO_4]$ tetrahedra have been observed in Ca_3SiO_5 [26]. In order to form the silicate network of corner-sharing $[SiO_4]$ tetrahedra during hydration process the intermediate state like $[H_2SiO_4]^{2-}$ should be indispensable. In case of Ca(1), we found the unusual valence of Ca(1) less than 2+ and suggested the existence of the $[Ca(1)SiO_4]^{2-}$ unit with covalency in β-Ca_2SiO_4. From these results, we could imagine a hydration process as follows. The $[Ca(1)SiO_4]^{2-}$ unit is substituted with two protons; $[CaSiO_4]^{2-} + 2H^+ \rightarrow [H_2SiO_4]^{2-} + Ca^{2+}$ (see Fig. 8). Subsequently, the silica chains are created by dehydroxylation of–OH on $[H_2SiO_4]^{2-}$, as proposed in investigations of hydroxyapatite [27]. In the meantime, Ca(2) is probably soluble as Ca^{2+} in water since the valence of Ca(2) is maintained as 2+ in β-Ca_2SiO_4. The Ca ions dissolved in water would be consumed to form C–S–H gel or to precipitate $Ca(OH)_2$.

Finally, although β-Ca_2SiO_4 has low heat of hydration, the hydration rate is generally slower than those of other components in cement clinkers [28]. Presumably, to control the Ca(1)–O(1) in the Ca(1)–$[SiO_4]$ unit is particularly significant for further improvement in hydration properties of β-Ca_2SiO_4.

4. Conclusion

Polycrystalline β-Ca_2SiO_4 could be obtained as a single-phase material. The crystal structure was refined on the basis of $P2_1/n$ symmetry (monoclinic) using TOF-NPD and the Rietveld method. It was validated that two different types of Ca sites, Ca(1) and Ca(2), exist in β-Ca_2SiO_4. The environments around Ca(1) and Ca(2) are markedly different; the coordination numbers of O atom around Ca(1) and Ca(2) for Ca–O bonds are 7 and 8 within 3 Å, respectively. The bond length distribution of Ca(1)–O is broader than that of Ca(2)–O, namely O atoms around Ca(1) distribute anisotropically in comparison with those around Ca(2). The bond length for each Ca–O was obtained, and then charge states of Ca(1) and Ca(2) were estimated as 1.87+ and 2+ by the Zachariasen–Brown–Altermatt formula (bond valence sum). In addition, it was found that the bond length of Ca(1)–O(1) in β-Ca_2SiO_4, is short and kept constant at 2.23 Å at a series of temperatures between RT and 600 °C. These results would lead to the important conclusion that the Ca(1)–O(1) has covalency whereas Ca(2) is in ionic condition. We strongly suggest that the solubility process of Ca ions into water should be different between two Ca sites; the intermediate states of Ca(1) and Ca(2) are the $[Ca(1)SiO_4]^{2-}$ unit with covalency on Ca(1)–O(1) and $Ca(2)^{2+}$, respectively.

Acknowledgments

We wish to acknowledge several useful discussions with Dr. K. Oishi of Shimizu Corporation and Prof. M. Kawai

of KENS at KEK. Many thanks are given to Dr. J. Fieramosca and Prof. J.W. Richardson of IPNS at ANL for valuable technical supports of TOF-NPD experiments. This work was supported by a Grant-in-Aid for Creative Scientific Research from the Ministry of Education, Science, Sports and Culture, Japan.

References

[1] C. Remy, B. Reynard, M. Madon, J. Am. Ceram. Soc. 80 (2) (1997) 413–423.
[2] W.G. Mumme, R.J. Hill, G. Bushnell-Wye, E.R. Segnit, N. Jb. Miner. Abh. 169 (1995) 35–68.
[3] W. Mumme, L. Cranswick, B. Chakoumakos, N. Jb. Miner. Abh. 170 (1996) 171–188.
[4] V. Peterson, B. Hunter, A. Ray, L.P. Aldride, Appl. Phys. A 74 (Suppl.) (2002) S1409–S1411.
[5] R. Berliner, C. Ball, P.B. West, Cem. Concr. Res. 27 (4) (1997) 551–575.
[6] F. Tzschichholz, H.J. Herrmann, H. Zanni, Phys. Rev. E 53 (1996) 2629–2638.
[7] S.A. FitzGerald, D.A. Neumann, J.J. Rush, D.P. Bentz, R.A. Livingston, Chem. Mater. 10 (1998) 397–402.
[8] A.J. Allen, J.C. McLaughlin, D.A. Neumann, R.A. Livingston, J. Mater. Res. 19 (11) (2004) 3242–3254.
[9] A.G. De la Torre, M.A.G. Aranda, J. Appl. Crystallogr. 36 (2003) 1169–1176.
[10] J.D. Jorgensen, J.J. Faber, J.M. Carpenter, R.K. Crawford, J.R. Haumann, R.L. Hittermann, R. Kleb, G.E. Ostrowski, F.J. Rotella, T.G. Worton, J. Appl. Crystallogr. 22 (1989) 321–333.
[11] H.M. Rietveld, J. Appl. Crystallogr. 2 (1969) 65–71.
[12] A.C. Larson, R.B. von-Dreele, Los Alamos National Laboratories, Report LAUR 86, 1994, p. 748.
[13] B.H. Toby, J. Appl. Crystallogr. 34 (2001) 210–213.
[14] N. Watanabe, T. Fukunaga, T. Shinohe, K. Yamada, T. Mizoguchi, in: Proceedings of ICANS-IV, KENS Report II, 1981, pp. 539–548.
[15] M. Misawa, T. Fukunaga, T. Yamaguchi, N. Watanabe, in: Proceedings of ICANS-IX, 1986, pp. 539–550.
[16] T. Fukunaga, M. Misawa, I. Fujikawa, S. Satoh, KENS Report-IX, 1993, pp. 16–17.
[17] H.H. Paalman, C.J. Pings, J. Appl. Phys. 33 (1962) 2635–2639.
[18] I.A. Blech, B.L. Averbach, Phys. Rev. 137 (1965) A1113–A1116.
[19] I.D. Brown, D. Altermatt, Acta Crystallogr. B 41 (1985) 244–247.
[20] N.E. Brese, M. O'Keeffe, Acta Crystallogr. B 47 (1991) 192–197.
[21] M. Yashima, A. Sakai, T. Kamiyama, A. Hoshikawa, J. Solid State Chem. 175 (2003) 272–277.
[22] S. Yamazaki, H. Toraya, J. Am. Ceram. Soc. 84 (11) (2001) 2685–2690.
[23] J.J. Chen, J.J. Thomas, H.F.W. Taylor, H.M. Jennings, Cem. Concr. Res. 34 (2004) 1499–1519.
[24] E. Bonaccorsi, S. Merlino, H.F.W. Taylor, Cem. Concr. Res. 34 (2004) 1481–1488.
[25] A. Nonat, Cem. Concr. Res. 34 (2004) 1521–1528.
[26] K. Mori, T. Fukunaga, Y. Shiraishi, K. Itoh, Q. Xu, K. Oishi, K. Yatsuyanagi, K. Iwase, M. Yonemura, M. Sugiyama, T. Ishigaki, T. Kamiyama, M. Kawai, Cem. Concr. Res., in press.
[27] F. Branda, R. Fresa, A. Costantini, A. Buri, Biomaterials 17 (1996) 2247–2251.
[28] V.K. Peterson, D.A. Neumann, R.A. Livingston, J. Phys. Chem. B 109 (2005) 14449–14453.